

Neutralization of Polyatomic Ions at Self-Assembled Monolayer Surfaces before and after Electrodeposition of Poly(phenylene oxide)

Thomas E. Kane,[†] Vincent J. Angelico,[‡] and Vicki H. Wysocki^{*‡}

Department of Chemistry, Virginia Commonwealth University, Richmond, Virginia 23284

Received April 8, 1997. In Final Form: October 8, 1997[⊗]

Self-assembled monolayer (SAM) films chemisorbed onto polycrystalline gold substrates have been shown to be effective targets in ion surface collision investigations. One concern has been whether localized defect sites within SAM films (pinholes) influence the amount of ion neutralization that occurs at the surface. Two molecular ion probes, benzene and DMSO-*d*₆, are employed to measure the degree of neutralization of a selected monolayer. In this investigation, the behavior of these probes upon collision with SAM surfaces composed of CH₃(CH₂)₃S-Au (C4), CH₃(CH₂)₁₇S-Au (C18), and CF₃(CF₂)₇(CH₂)₂S-Au (CF) is compared to the behavior of the same SAM surfaces after potential defect sites have been modified by electrodeposition of poly(phenylene oxide). Plots of total ion current vs time show no change in the scattered ion efficiency as a result of the chemical treatment for any of the monolayer films, even in the case of C4 where the CV electrodeposition experiments indicate exposed gold. The results indicate that neutralization of the ion beam that occurs for each SAM film is not a result of the presence of defect sites within the monolayer films. Furthermore, the results also suggest that the C18 and CF surfaces used routinely in surface-induced dissociation experiments in this laboratory do not contain a significant number of defect sites that expose gold.

Self-assembled monolayer (SAM) films of alkanethiolates chemisorbed onto gold substrates represent stable, organic materials that have been shown to be effective targets for ion surface collision experiments in vacuum.¹⁻¹⁰ Fragmentation spectra yielding structural information for a variety of mass selected projectile ions have been obtained via low-energy (<100 eV) surface collisions in the process referred to as surface-induced dissociation (SID).¹¹⁻²⁰ Neutralization of odd electron projectile ions at the surface can be a dominant reaction pathway for

unmodified metal surfaces and some SAM films. Neutralization can be indirectly measured as the ratio of total ion current after the surface collision versus the initial incident ion current. The amount of detectable scattered ion signal with respect to the initial ion signal is referred to here as the scattered ion efficiency and is the primary focus of this paper. Scattered ion efficiency values have been reported for various *n*-alkanethiolate SAM films, namely, CH₃(CH₂)_{*n*}S-Au (*n* = 3, 7, 11, 17) and CF₃(CF₂)₇(CH₂)₂S-Au.⁶ Common efficiency values measured in this laboratory for a variety of molecular ions are 3-15% for hydrocarbon SAM films and 60-70% for fluorinated SAM films.⁶ Although different groups have reported different absolute values for efficiency, most report the same general trends.¹⁰ The trends observed include an increase in scattered ion efficiency (less neutralization) of molecular ions for *n*-alkanethiolate hydrocarbon SAM films with increasing methylene chain length and consistently greater efficiency values for fluorinated alkanethiolates, as compared to hydrocarbon-based films.

Several explanations have been proposed for the observed trends in scattered ion efficiency when SAM films are used as collision targets. The dramatically different efficiency values for hydrocarbon versus fluorinated films suggest that electron transfer from surface chains is one of the main pathways involved in ion neutralization, but other pathways might also contribute.²¹ The possibility exists that ion neutralization may occur at localized regions of incomplete monolayer formation that are known to be present, albeit at low concentrations, within monolayer films (e.g., see Figure 1b). Pinholes or other defect sites that expose the gold substrate might act as sites

[†] Present address: Premier American Technologies Corp., 1155 Zion Road, Bellefonte, PA 16823.

[‡] Present address: Department of Chemistry, University of Arizona, Tucson, AZ 85721.

[⊗] Abstract published in *Advance ACS Abstracts*, November 15, 1997.

(1) Winger, B. E.; Julian, R. K., Jr.; Cooks, R. G.; Chidsey, C. E. D. *J. Am. Chem. Soc.* **1991**, *113*, 8967.

(2) Wysocki, V. H.; Jones, J. L.; Ding, J. *J. Am. Chem. Soc.* **1991**, *113*, 8969.

(3) Morris, M.; Riederer, D. E., Jr.; Winger, B. E.; Cooks, R. G.; Ast, T.; Chidsey, C. E. D. *Int. J. Mass Spectrom. Ion Processes* **1992**, *122*, 181.

(4) Winger, B. E.; Laue, H.-J.; Horning, S. R.; Julian, R. K., Jr.; Lammert, S. A.; Riederer, D. E., Jr.; Cooks, R. G. *Rev. Sci. Instrum.* **1992**, *63*, 5613.

(5) Callahan, J. H.; Somogyi, Á.; Wysocki, V. H. *Rapid Commun. Mass Spectrom.* **1993**, *7*, 693.

(6) Somogyi, Á.; Kane, T. E.; Ding, J. M.; Wysocki, V. H. *J. Am. Chem. Soc.* **1993**, *115*, 5275.

(7) Kane, T. E.; Somogyi, Á.; Wysocki, V. H. *Org. Mass Spectrom.* **1993**, *28*, 1665.

(8) Somogyi, Á.; Kane, T. E.; Wysocki, V. H. *Org. Mass Spectrom.* **1993**, *28*, 283.

(9) Kane, T. E.; Angelico, V. J.; Wysocki, V. H. *Anal. Chem.* **1994**, *66*, 21, 3733.

(10) Schey, K. L.; Durkin, D. A.; Thornburg, K. R. *J. Am. Soc. Mass Spectrom.* **1995**, *6*, 257.

(11) Cooks, R. G.; Ast, T.; Mabud, Md. A. *Int. J. Mass Spectrom. Ion Processes* **1990**, *100*, 209.

(12) McCormack, A. L.; Somogyi, Á.; Dongré, A. R.; Wysocki, V. H. *Anal. Chem.* **1993**, *65*, 2857.

(13) Wysocki, V. H.; Jones, J. L.; Dongré, A. R.; Somogyi, Á.; McCormack, A. L. In *Biological Mass Spectrometry: Present and Future*; Matsuo, T., Caprioli, R. M., Gross, M. L., Seyama, Y., Eds.; John Wiley and Sons: New York, 1994; p 249.

(14) Bier, M. E.; Schwartz, J. C.; Schey, K. L.; Cooks, R. G. *Int. J. Mass Spectrom. Ion Processes* **1990**, *103*, 1.

(15) Wysocki, V. H.; Ding, J. M.; Jones, J. L.; Callahan, J.; King, F. L. *J. Am. Soc. Mass Spectrom.* **1992**, *3*, 27.

(16) Williams, E. R.; Jones, G. C., Jr.; Fang, L.; Zare, R. N.; Garrison, B. J.; Brenner, D. W. *J. Am. Chem. Soc.* **1992**, *114*, 3207.

(17) Beck, R. D.; St. John, P.; Alvarez, M. M.; Diederich, F.; Whetten, R. L. *J. Phys. Chem.* **1991**, *95*, 8402.

(18) Bier, M. E.; Amy, J. W.; Cooks, R. G.; Syka, J. E. P.; Ceja, P.; Stafford, G. *Int. J. Mass Spectrom. Ion Processes* **1987**, *88*, 31.

(19) Dongré, A. R.; Somogyi, Á.; Wysocki, V. H. *J. Mass Spectrom.* **1996**, *31*, 339.

(20) Dongré, A. R.; Jones, J. L.; Somogyi, Á.; Wysocki, V. H. *J. Am. Chem. Soc.* **1996**, *118*, 8365.

(21) Wainhaus, S. B.; Burroughs, J. A.; Hanley, L. *Surf. Sci.* **1994**, *344*, 122.

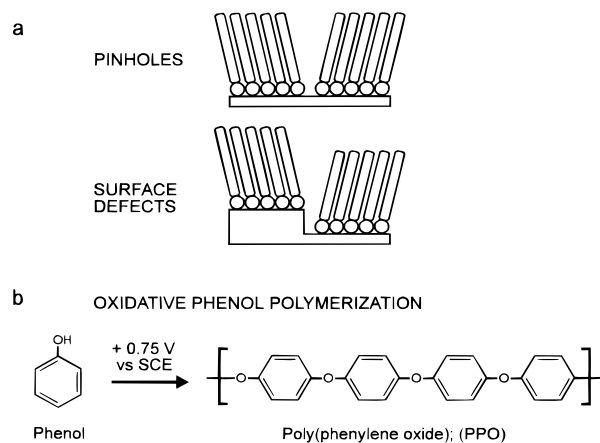


Figure 1. (a) Illustration of monolayer pinholes and surface defects. (b) Electrochemical oxidation of phenol to poly(phenylene oxide).

where ion neutralization could occur with greater probability than at the organic layer. The presence of pinholes in monolayer films has been reported from scanning tunneling microscopy (STM)^{22–25} as well as atomic force microscopy (AFM)²⁶ investigations. The effects of pinholes on electrochemical rates of reaction have been studied in solution by reversible redox couple compounds such as $[\text{Fe}(\text{CN})_6]^{3+/2+}$ and $[\text{Ru}(\text{NH}_3)_6]^{3+/2+}$.^{27–31} The relative surface area occupied by pinholes has been measured by electrochemical gold oxide stripping,^{27,31,32} and individual sizes and populations have been estimated with microelectrode model calculations applied to the currents measured with the redox couple compounds.^{27,31,33} Values for the average pinhole fraction range from 10^{-2} to 10^{-5} and estimated sizes range from 350 to 2000 Å², depending on the monolayer thiolate chain length, with the fraction decreasing as the chain length of the film increases.^{27,31,33}

Low concentrations of phenol in acidic aqueous solutions have been shown to promote thin film coatings of poly(phenylene oxide) (PPO, see Figure 1b) on unmodified electrodes^{34–38} and specifically at defect sites when the electrochemical reaction is performed on SAM-coated electrodes.³⁰ Finklea has shown with cyclic voltammetry and ellipsometric techniques that, under aqueous and slightly acidic solution conditions, the phenol polymerization is predominantly localized at the pinhole sites.³⁰ Ellipsometric measurements by Finklea also suggest that the polymerization process does not appreciably alter the thickness of the monolayer. After an adequate amount

of time the cyclic voltammogram (CV) scans indicate complete polymerization of the surface at defect sites, and no further current flow is observed.

This paper describes a series of tandem mass spectrometry surface-induced dissociation experiments that compare SAM films that have been electrochemically modified by polymerization of poly(phenylene oxide) to SAM films that have not been modified. Benzene (m/z 78) and DMSO- d_6 (m/z 84) are used as the molecular ion probes and have been previously shown to be effective for measurements of scattered ion efficiency and ion surface reactions.^{6–9} The monolayer films utilized are prepared from $\text{CH}_3(\text{CH}_2)_3\text{SH}$, $\text{CH}_3(\text{CH}_2)_{17}\text{SH}$, and $\text{CF}_3(\text{CF}_2)_7(\text{CH}_2)_2\text{-SH}$ chemisorbed onto gold substrates and are referred to as C4, C18, and CF surfaces, respectively. The lack of significant current flow during the electrodeposition step will be taken as evidence that only limited amounts of exposed metal exist as potential neutralization sites. Any change in the scattered ion efficiency behavior of the surfaces before and after electrodeposition will be associated with the presence of pinholes.

Experimental Section

The SAM preparation method employed by this laboratory follows standard procedures and has been described elsewhere.⁶ For the monolayer modification, a standard three-electrode electrochemical cell was constructed in a 50 mL flat-bottomed Pyrex cylinder with a Teflon cap. A 50 mM aqueous solution of phenol (Aldrich 99+%) was prepared in 0.5 M H_2SO_4 . A laboratory built Ag/AgCl reference electrode was prepared (3 M KCl), and a coiled platinum wire was used as a counter electrode. To reduce the possibility of polymer formation on the counter electrode, it was encapsulated in a tube with a fritted glass bottom (Ace glass, 25–50 μm pore size) containing 0.5 M H_2SO_4 . The SAM surface was placed on the bottom of the electrochemical cell and connected to a wire lead, which passed up through the cell. Contact was made approximately 2 mm away from one of the corners of the gold surface. A frame assembly on the surface holder in the mass spectrometer masks this region. As a means of characterizing the cell, standard CV scans of 50 mM $\text{K}_3\text{Fe}(\text{CN})_6$ in 1.0 M KNO_3 were performed prior to the phenol polymerization, with a second platinum coil used as a working electrode in place of the SAM surface. After extensive rinsing of the cell and its components in deionized water, a background scan confirming the removal of the $\text{K}_3\text{Fe}(\text{CN})_6$ was taken prior to the introduction of the SAM surface to the phenol solution. The potential scan range for the polymerization of the phenol is 0.0 to +1.0 V vs Ag/AgCl (potentials greater than +1.4 V result in the desorption of the monolayer from the gold substrate³⁰). A commercial CV potentiostat (BAS cyclic voltammetry, Model CV-1B) was ramped at a 50 mV/s scan rate. The data were obtained with a MFE 815 Plotmatic analog recorder. Repeated CV sweeps from 0.0 to +1.0 V were employed to polymerize the phenol and to determine the extent of the monolayer polymerization (10 CV cycles). The modified surfaces are removed from the electrochemical cell, gently rinsed in a clean ethanol stream for approximately 10 s, and immediately mounted and introduced into the vacuum chamber.

SID Using Self-Assembled Monolayers. The mass spectrometer configuration has been described in detail elsewhere.¹⁵ Two Extrel 4000u quadrupoles (Q1 and Q2) are arranged in a 90° geometry with a surface placed to intersect the ion optical path. The surface is positioned at a 45° angle relative to the ion beam exiting from Q1. Increasing the ion source potential relative to the surface potential varies the collision energy. Ions are transmitted past the surface without collision by setting the potential difference between the ion source and the surface at approximately 0 V. A multiple surface holder has been designed to allow for the use of up to six surfaces without venting the instrument. The holder is an 18 mm by 160 mm ceramic strip at the tip of a movable rod, with individual stainless-steel frames (Kimball Physics, Wilton, NH) holding each surface in place. The holder is affixed vertically, allowing any of the six surfaces to be positioned in the path of the ion beam. The surfaces are electrically linked via the back of the holder, and a single power

(22) Kim, Y. T.; Bard, A. J. *Langmuir* **1992**, *8*, 1096.

(23) Edinger, K.; Golzhauser, A.; Demota, K.; Woll, Ch.; Grunze, M. *Langmuir* **1993**, *9*, 4.

(24) Sun, L.; Crooks, R. M. *Langmuir* **1993**, *9*, 1951.

(25) Ross, C. B.; Sun, L.; Crooks, R. M. *Langmuir* **1993**, *9*, 632.

(26) Alves, C. A.; Smith, E. L.; Porter, M. D. *J. Am. Chem. Soc.* **1992**, *114*, 1222.

(27) Finklea, H. O.; Avery, S.; Lynch, M.; Furtch, T. *Langmuir* **1987**, *3*, 409.

(28) Chidsey, C. E. D.; Loiacono, D. N. *Langmuir* **1990**, *6*, 682.

(29) Li, T. T.; Weaver, M. J. *J. Am. Chem. Soc.* **1984**, *106*, 6107.

(30) Finklea, H. O.; Snider, D. A.; Fedyk, J. *Langmuir* **1990**, *6*, 371.

(31) Finklea, H. O.; Hanshew, D. D. *J. Am. Chem. Soc.* **1992**, *114*, 3173.

(32) Creager, S. E.; Hockett, L. A.; Rowe, G. K. *Langmuir* **1991**, *8*, 854.

(33) Miller, C.; Cuendet, P.; Gratzel, M. *J. Phys. Chem.* **1992**, *95*, 877.

(34) Siepmann, J. I.; McDonald, I. R. *Langmuir* **1993**, *9*, 2351.

(35) Bejerano, T.; Forgacs, C.; Gileadi, E. *J. Electroanal. Chem.* **1970**, *27*, 69.

(36) Zeigerson, E.; Gileadi, E. *J. Electroanal. Chem.* **1970**, *28*, 421.

(37) Bruno, F.; Dubois, J. E. *Electrochim. Acta* **1972**, *17*, 1161.

(38) Bruno, F.; Pham, M. C.; Dubois, J. E. *Electrochim. Acta* **1977**, *22*, 451.

supply is used to apply an equivalent potential to each of the surfaces. Experimental results suggest that the instrument tuning parameters do not change noticeably when the surface positioned in the ion path is changed from one to another. The advantage to having more than one surface in the instrument at any given time is that the instrument parameters will remain constant during investigations requiring more than one type of surface (e.g., no venting, no retuning, limited pressure fluctuations, etc.). The surface can also be rotated about the z -axis (Q1 and Q2 are in the x - y plane).

Measuring the Scattered Ion Efficiency: Total Ion Current Measurements (TICs). When the instrument is operating in the MS/MS mode to obtain SID spectral data for a selected incident ion, the second quadrupole (Q2) behaves as a scanning mass filter. The Q2 spectrum range (10–150 Da) includes the molecular mass of the incident ion, as well as fragments, reaction products, and sputtered species resulting from the ion surface collisions.⁶ The data system reports the ion flux that passes through Q2 as a continuous current vs time signal, which represents the sum of all the spectral peak intensities present within the scan range. This raw data, without first being deconvoluted to the individual peaks in the mass spectrum, is plotted as a single line (total ion current, TIC) and describes the total signal intensity of the mass spectrum (using a given target surface) versus time.

Direct comparison of the TIC intensity of one monolayer surface to another under equivalent experimental conditions represents a *relative* measure of the scattered ion efficiency between monolayer surface types. The multiple surface holder allows the surfaces to be switched without alteration to the instrument tuning, sample pressure, and multiplier gain. The resulting data are graphic illustrations of the differences in signal intensity for the different monolayer surfaces.

Results and Discussion

Cyclic Voltammetry: Evidence of Polymerization.

C4, C18, and CF monolayer surfaces were modified by electrodeposition of poly(phenylene oxide) and introduced into the tandem mass spectrometer along with an equivalent series of unmodified monolayer surfaces. Parts a–c of Figure 2 illustrate the initial CV plots of the PPO polymerization for the C4, C18, and the CF monolayer surfaces. The current that is observed from the C4 surface beginning at 0.75 V represents the oxidation of the phenol. The initial CV shape is nearly identical to the plot presented by Finklea for poly(phenylene oxide) deposition onto an unmodified gold electrode.³⁰ The current density measured during the second scan (not shown) is reduced to roughly one-tenth that of the first scan, suggesting rapid polymerization of the exposed gold. The surfaces were subjected to eight additional CV potential sweeps, the last (tenth) for each monolayer being illustrated in Figure 2d–f. After 10 complete cycles with the C4 surface, no appreciable Faradaic current is observed, suggesting polymerization at exposed gold on the surface and successful blocking of pinholes or defect sites. The C18 monolayer exhibited a small current at the outset suggesting more complete coverage of the gold substrate and fewer defect sites than the C4 surface. The CF monolayer is essentially current free suggesting that pinholes are absent or in low enough concentration that they are undetectable in the voltammogram. Chidsey has shown cyclic voltammograms for solutions of $\text{Ru}(\text{NH}_3)_6\text{Cl}_3$ and $\text{K}_3\text{Fe}(\text{CN})_6$ using $\text{CF}_3(\text{CF}_2)_7(\text{CH}_2)_2\text{S}-\text{Au}$ and $\text{CH}_3(\text{CH}_2)_9\text{S}-\text{Au}$ monolayer coated electrodes²⁸ where the current associated with the reduction of the ruthenium or the iron complex was negligible, suggesting the monolayers effectively contained no pinholes. The CV plots presented here support those claims, and after 10 successive CV sweeps, no change was observed in the plots. Figure 2d–f suggests that after the electrodeposition the surfaces are largely equivalent in that none of them contain an appreciable amount of exposed gold.

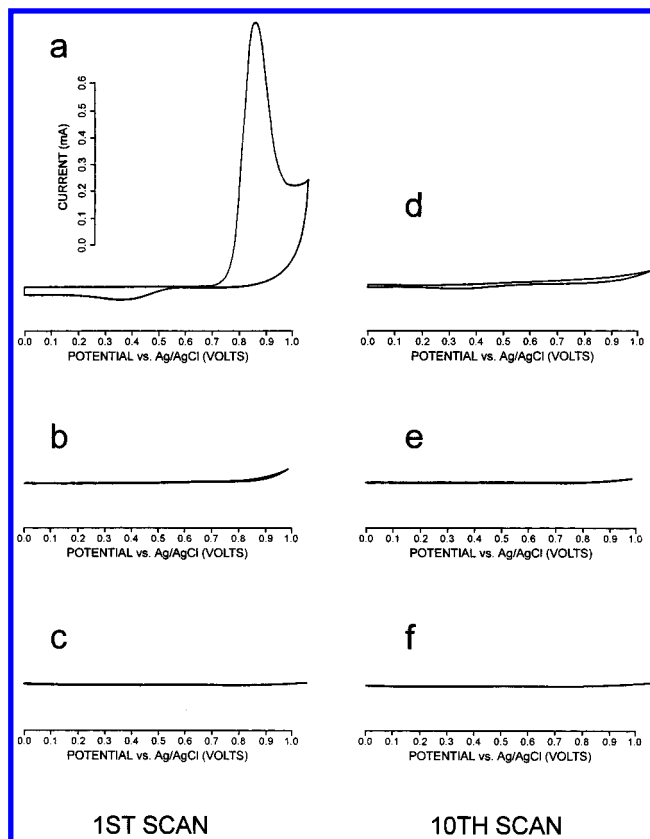


Figure 2. Cyclic voltammograms depicting the oxidation deposition of poly(phenylene oxide) on (a) $\text{CH}_3(\text{CH}_2)_3\text{S}-\text{Au}$ surface, first CV sweep, (b) $\text{CH}_3(\text{CH}_2)_{17}\text{S}-\text{Au}$ surface, first CV sweep, and (c) $\text{CF}_3(\text{CF}_2)_7(\text{CH}_2)_2\text{S}-\text{Au}$ surface, first CV sweep. Cyclic voltammograms depicting the tenth CV sweep on (d) $\text{CH}_3(\text{CH}_2)_3\text{S}-\text{Au}$ surface, tenth CV sweep, (e) $\text{CH}_3(\text{CH}_2)_{17}\text{S}-\text{Au}$ surface, tenth CV sweep, and (f) $\text{CF}_3(\text{CF}_2)_7(\text{CH}_2)_2\text{S}-\text{Au}$ surface, tenth CV sweep.

Efficiency Measurements: Comparison of Monolayer Surfaces. After electrodeposition of the polymer, the modified C4, C18, and CF surfaces were introduced into the vacuum chamber accompanied by three unmodified SAM surfaces. Each surface was successively moved into the ion optical path without changes to the instrument tuning or pressure. Benzene and $\text{DMSO}-d_6$ were collided into each of the modified monolayer surfaces, and the scattered ion efficiency plots and surface-induced dissociation spectra (not shown) were compared to those obtained from unmodified SAM films. The total ion current plot obtained for collisions of benzene molecular ion with each of the surfaces is given in Figure 3. The plotted signal represents the total ion current reaching the detector, when each of the selected surfaces is positioned in the ion beam path. The efficiency results obtained using ion probes of known chemical behavior are a confirmation that no severe alteration of the modified monolayers has occurred, due either to the time spent in an acidic phenol solution or to possible mechanical damage incurred by the electrochemical cell setup. The six intensities represent the signals obtained with the six individual surfaces, measured over several minutes. The values represented graphically in Figure 3 for the relative efficiency of charge retention of benzene, measured at the unmodified SAM surfaces, are in agreement with those previously published.⁶ As noted before, longer chain alkanethiolates demonstrate less neutralization than shorter chains, and fluorinated alkanethiolates lead to less neutralization than long chain (i.e., C18) alkanethiolates.

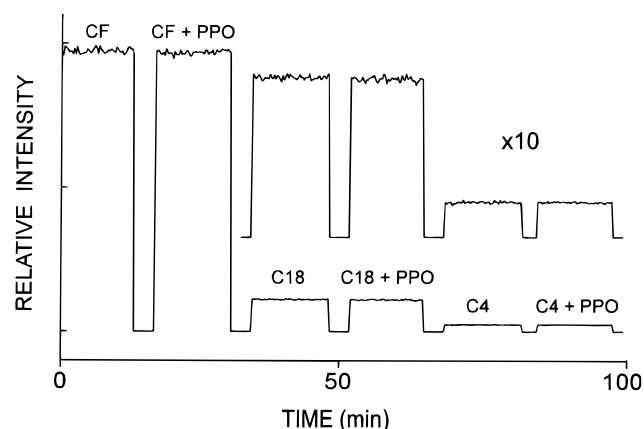


Figure 3. Total ion current (TIC) plot of the 30 eV collision of benzene molecular ion on unmodified and PPO modified monolayer coated gold surfaces.

It is clear from Figure 3 that blocking defect sites within the monolayers had no significant effect on the amount of signal observed for benzene at 30 eV. Similar results were obtained for 20 eV collisions of DMSO- d_6 (not shown). Efficiencies measured as TIC values, and as ratios of the scattered ion versus the incident ion current, are nearly identical for both modified and unmodified monolayers. Neutralization of the ions at pinholes or defect sites within the monolayer film does not appear to be an appreciable contributor to signal loss. *This suggests that the relative thickness of the films, and not exposed gold, plays a role in the neutralization for C4 and C18.* An additional factor, e.g., the ionization energy of the surface chains, is important in comparisons of the C18 and CF surfaces,

which are of similar thickness.³⁹ It is also possible that adventitious hydrocarbons known to be present in the vacuum chamber could be coating any exposed gold or pinholes that might be present in the untreated monolayer films.⁷ This could cause the unmodified monolayer films to give similar efficiency values to those that were treated with the poly(phenylene oxide).

Conclusions

The oxidation current observed at the appropriate voltage (+0.75 mV vs SCE) for the C4 monolayer surface in solution confirms the polymerization by electrodeposition of PPO at defect sites. Little or no current is observed for the C18 and CF monolayer surfaces, indicating few defect sites with exposed gold. It is clear that for the surfaces used routinely in this laboratory as targets in SID experiments, pinholes and or defect sites do not play a significant role in ion neutralization. The results suggest that the film thicknesses and the ionization energy of the surface chains are the primary factors influencing neutralization.

Acknowledgment. Funding provided by the National Science Foundation (Grant Number CHE-9224719). We thank Dr. Fred Hawkrige of Virginia Commonwealth University for helpful discussions on the electrochemical processes reported here and for the use of the potentiostat and analog recorder.

LA9703611

(39) Kane, T. E. Dissertation, Surface-induced dissociation at self-assembled monolayer films: characterization and measurement of ion-surface interactions; 1995, Virginia Commonwealth University, Richmond, VA.